J Mater Sci (2010) 45:706–712
DOI 10.1007/s10853-009-3988-4

Electrokinetic properties of Nd:YAG nanopowder and a high concentration slurry with ammonium poly(acrylic acid) as dispersant

**Yao-Hui Lv · Hong Liu · Yuan-Hua Sang ·
Shu-Jiang Liu · Ting Chen · Hai-Ming Qin ·
Ji-Yang Wang**

Received: 31 July 2009 / Accepted: 20 October 2009 / Published online: 6 November 2009

Abstract The electrokinetic properties of Nd:YAG nanopowder with particles of about 40 nm in diameter were investigated by measuring the zeta potential of a stable YAG ($Y_3Al_5O_{12}$) aqueous slurry. Ammonium poly(acrylic acid) polyelectrolyte was used as dispersant to adjust the electrokinetic properties of the Nd:YAG slurry. The effect of the pH of the slurry and of the polyelectrolyte concentration on the stability of the suspension are discussed in this study. The optimal pH value and the amount of dispersant needed to obtain a stable Nd:YAG nanoparticle slurry were determined. Highly consistent Nd:YAG nanoparticle slurries with optimal pH and dispersant concentration were prepared by ball milling. The rheological behavior of Nd:YAG slip with different solid loading (60–70 wt%) has been studied by measuring the viscosity and shear stress as a function of shear rate. Slip with solid loadings of 65 wt% shows near-Newtonian behavior but becomes non-Newtonian with typical shear-thinning behavior above this solid loading value. The density and microstructure of the cast product bears a direct relationship to the state of the slip induced by alternation of the pH and the concentration of the dispersant as well as the solid loading.

Introduction

Transparent yttrium aluminum garnet ($Y_3Al_5O_{12}$) ceramic is an important laser material with excellent chemical stability, good optical and thermal properties, and high temperature creep resistance. It has proved to be one of the most promising laser materials for many kinds of laser devices, especially high power lasers [1–3]. Many factors, such as the purity of the raw materials, grain boundary thickness, ceramic porosity, etc., affect the transparency and laser properties of the ceramic. Among these factors, the number and size of micropores are the most important factors governing the optical and laser properties because of the scattering loss caused by the interface between the air in the pores and the ceramic substrate. Lowering the porosity of the ceramic is therefore the greatest challenge to improving the laser properties of YAG. Although there are three different YAG ceramic fabrication processes, including nanoparticle preparation, green body formation, and sintering, in attempting to control the porosity of the ceramic, the effect of the formation process is often ignored. The reported YAG formation methods are usually dry-pressing [4–10], iso-static pressing [11, 12], and a few reports that indicate using the slip casting method [13–18]. Generally speaking, using a green body obtained from a press formation method makes it difficult to obtain a pore-free ceramic with vacuum sintering because some large pores presents during the formation process under high pressure [19]. Compared to the press formation method, with a green body formed from the slip casting method it should be easier to obtain a dense ceramic because all the pores in the green body from the slip casting method originate from discharge in the dispersion medium. Therefore, the air in the connected channels can be more easily pumped out during vacuum sintering.

Based on this advantage, slip casting, which is an ancient formation method, has been intensively applied to the fabrication of transparent and other advanced ceramics [20–24]. If the goal is the fabrication of a pore-free

Y.-H. Lv · H. Liu (✉) · Y.-H. Sang · S.-J. Liu · T. Chen ·
H.-M. Qin · J.-Y. Wang
State Key Laboratory of Crystal Materials, Shandong University,
Jinan 250100, China
e-mail: hongliu@sdu.edu.cn

transparent YAG ceramic, a uniform green body with high density is necessary. However, because Nd:YAG particles are of nanometer size, the slurry properties of the Nd:YAG powder are quite different from the clay suspension, a condition that presents a great obstacle to obtaining highly loaded Nd:YAG slurries.

As is well known, slip casting is based on a traditional formation process: a ceramic powder is dispersed in a dispersion medium, forms a slurry and is poured into a porous mold; the dispersion medium is expelled from the slurry under the capillary action of the mold, and a solid green body is obtained. Therefore, the characteristics of the ceramic slurry are the most important factor for the fabrication of a uniform high density green body. The ceramic slurry must satisfy the following conditions to obtain a highly dense green body: (1) high solid content, (2) low viscosity, and (3) good dispersion [25–27]. A satisfactory slurry can be obtained by choosing a suitable dispersant of critical concentration and proper pH [28]. The principle of stabilization by electrostatic repulsion is described by the Derjaguin–Landau–Verwey–Overbeek (DLVO) theory. Stabilization is possible only when the repulsive forces are greater than the attractive forces. The stabilization of electrostatic repulsion depends on both the radius of the particles and their surface potential, ψ_0. This latter parameter depends directly on the surface charges and is independent of the grain size of the powder [29]. The zeta potential corresponds to the charge of a colloidal particle in the proximity of its surface, and is generally used as a quantitative measurement to predict suspension stability. The value zeta potential = 0 is the isoelectric point (IEP), at which repulsion forces disappear and flocculation occurs. On the other hand, a higher zeta potential value results in higher repulsive forces and a more stable suspension. The value of zeta potential depends directly on the pH of the slurry and on the dispersant concentration, as well as on the nature of the particles in the slurry. Polyelectrolytes are usually added as dispersants to enhance slurry stability and modify the rheology in the colloidal processing of ceramics. The electrical double-layer thickness (Debye length) in a suspension, which is one of the most important processing parameters, is usually much smaller than the polymer adsorption layer thickness [30]. Other characteristic values, i.e., the Hamaker constant of the particles, the radius of the particles, and the electrostatic double-layer thickness, are thought to be changed by the adsorption of the polymer. Therefore, the dispersant concentration is assumed to have an extremely strong effect on the value of the zeta potential. The effect of pH and dispersant concentration on the zeta potential is the basis of the research on the cast formation of advanced ceramics.

In the present work, the effort is focused on investigating the effect of pH and dispersant concentration on the zeta potential with an average grain size of 40 nm. Based on a determination of the optimal parameters, the rheology of Nd:YAG slurries with different solid content was investigated. A uniform Nd:YAG green body with high solid content was prepared that was appropriate for the preparation transparent Nd:YAG ceramic. The green body was thoroughly characterized in terms of its microstructure and density.

Experimental

Nd:YAG powder of about 40 nm in diameter was synthesized by a co-precipitation method [31]. In order to control the dispersion of the nanopowder, an appropriate amount of $(NH_4)_2SO_4$ was added to the reactant solution during the synthesis. The dispersant used in this study was an NH_4^+ salt of poly(acrylic acid) (NH_4PAA) (30 wt%, Shanghai Reagents Co.).The morphology of the precursor and the Nd:YAG nanopowder was characterized by transmission electron microscopy (TEM, 100CXII, JEOL, Tokyo, Japan).

A Zeta potential analyzer, (Zetapals, Brookhaven Instruments Corporation, USA) was used to characterize the electrokinetic properties of the Nd:YAG nanoparticles. For the zeta potential measurement a Nd:YAG suspension of 2 mg/mL concentration was prepared by dispersing Nd:YAG powder in deionized water under continuous magnetic stirring. The effect of pH (in the range of 2–12) on the electrokinetic properties of the Nd:YAG powder was investigated in measuring the zeta potential by adjusting the pH of the suspension with the addition of 0.1 M HNO_3 for the acidic range, and 0.1 M sodium hydroxide (NaOH) solution for the alkaline range. The effect of adding NH_4PAA on the electrokinetic properties of the Nd:YAG suspension was explored by measuring the zeta potential of the suspension with different concentrations of NH_4PAA at a fixed pH (10.5).

To verify the relationship between the suspension properties and the zeta potential of the Nd:YAG nanopowder, the static settlement test was used to study the effects of the addition of dispersant to a stable Nd:YAG water slurry. 20 wt% solid-loaded Nd:YAG suspensions with different dispersant concentrations were milled for 3 h before allowing them to stand in a 25 mL graduated cylinder. The initial height of the suspension in the graduated cylinder was measured as H_0. The graduated cylinders were undisturbed for 7 days, and the height of the cloudy suspensions was measured as H_f.

Rheological measurements are typically used to characterize the behavior of fluid materials subjected to deformation strains [32], defined as the shear rate, $\dot{\gamma}$. The rheological behavior of a fluid is described by one of two flow curves: τ (shear stress) $= f(\dot{\gamma})$ or η (viscosity) $= f(\dot{\gamma})$. Highly solid-loaded Nd:YAG powder slurries (60, 65, 70 wt%) with optimal pH and an additional amount of NH_4PAA were carefully prepared by adding a fixed amount of Nd:YAG powder into a fixed volume of water of optimal pH and an additional amount of NH_4PAA. The mixture was then ball milled for rheological behavior measurements. The rheological behavior was studied by measuring their viscosity and shear stress as a function of shear rate on a rheometer (HAAKE RheoStress RS75, Germany). The measurements were performed at a constant temperature of 25 °C using a cylindrical configuration.

The suspensions with the highest solid content while at the same time retaining a low viscosity were subsequently slip cast in Plaster of Paris molds to form green bodies measuring 20 mm in diameter by 3 mm in thickness. The density of the formed green bodies was measured by the Archimedes method using kerosene. The fracture surfaces of the green samples were examined by using field emission scanning electron microscopy (SEM, S-4800, Hitachi, Tokyo, Japan).

Results and discussion

Figure 1a shows that the precursor particles are well-dispersed and nearly spherical with an average size of about 30 nm. The particle size of the as-synthesized Nd:YAG powder is about 40 nm (Fig. 1b). The particles are well dispersed probably because of the use of $(NH_4)_2SO_4$ as a dispersant during the synthesis and calcining process [33].

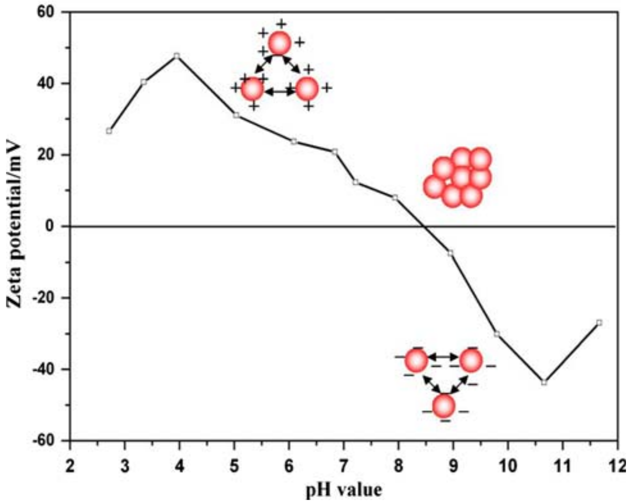

Fig. 2 Effect of pH on the zeta potential of Nd:YAG nanopowder in aqueous solution ($T = 25$ °C)

Figure 2 shows the result of zeta potential measurements for a series of aqueous Nd:YAG suspensions of different pH values. All the measured potential values are positive at low pH, then decrease with increasing pH, reach zero, and then become negative, and continue to decrease with further increase in the pH of the suspension. It is clear that the IEP (i.e., the pH at which the net charge on the particle surface is zero) for the as-received suspension was about pH 8.5, which is similar to the value reported in the literature [34]. This result is in agreement with the model for hydroxide groups adsorbed onto the surfaces of the particles. According to the literature, metal ions on the surface oxide layer behave as a Lewis acid [35]. In the case of aqueous slurries of oxides, a surface reaction results in the formation of amphoteric hydroxide groups, such as M–OH, which can dissociate as weak acids or bases [29]

$$\mathrm{M{-}OH(surface)} \leftrightarrow \mathrm{M{-}O^{-}(surface)} + \mathrm{H^{+}} \quad \text{(in basic slurries)} \tag{1}$$

$$\mathrm{M{-}OH(surface)} + \mathrm{H^{+}} \leftrightarrow \mathrm{M{-}OH_2^{+}(surface)} \quad \text{(in acid slurries)} \tag{2}$$

Below the IEP, adsorption of H^+ ions leads a positively charged surface, whereas above the IEP, the adsorption of

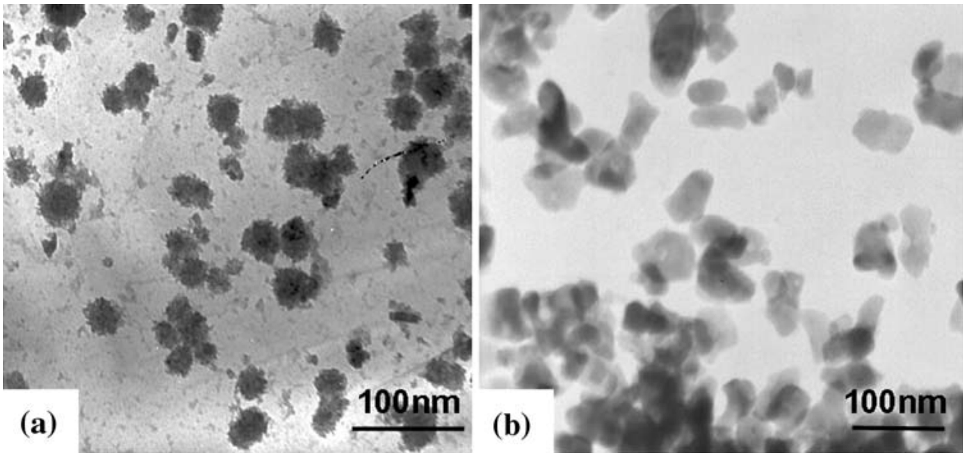

Fig. 1 TEM photograph of the precursor powder (**a**) and as-synthesized Nd:YAG powder (**b**) by co-precipitation method

OH^- ions produces a negatively charged surface. Pure alumina and yttrium oxide particles display isoelectric points in the pH range of ~8.5–9.5 and ~10.5–11, respectively [36–38], which implies that a fruitful comparison of the surface of the synthesized Nd:YAG powder can be made with pure alumina.

Generally, the zeta potential depends on the amount of H^+ or OH^- adsorbed on the particle surfaces and on the thickness of the double electron layer on the particle in suspension. In the Nd:YAG nanoparticle–water system, the starting positive value of the zeta potential is due to the adsorption of protons from the solution in which they are dispersed. At pH = 2, the overabundant adsorption of H^+ on the particle surfaces causes a compression of the double electron layer, which in turn produces a smaller zeta potential. The double electron layer decreases with the increase of the pH of the suspension, and reaches a maximum at a pH of about 4. At this point, the zeta potential is at its maximum value (48 mV). In such a system, the repulsive force between the particles caused by the positive surface charges reaches a maximum, and the suspension is in a very stable situation. With the increase of the pH, due to the decrease in the adsorption of protons from solution, the zeta potential gradually decreases and reaches the IEP at a pH of about 8.5. At the IEP, the amount of adsorption of H^+ is zero or better, and the adsorption of H^+ and OH^- ions on the particle surfaces are almost equal, so the zeta potential is zero. At this point, the slurry is very unstable, and agglomeration of the particles occurs even in a low load content Nd:YAG slurry. The adsorption of OH^- from solution on the nanopowder surfaces leads to a negative zeta potential value when the pH goes beyond the IEP. The amount of OH^- adsorbed on the surface of the nanoparticles increases with the increase in pH, which brings about an increase in the zeta potential of the particles. At pH = 10.5, the amount of OH^- adsorbed on the nanoparticle surfaces reaches a maximum, and the zeta potential reaches its minimum value (−43 mV). At this pH, the repulsive force on the particles is caused by the negative charges adsorbed on the particle surfaces. This state is also stable. Above a pH of 10.5, the compression of the double electron layer leads to a slight increase in the zeta potential because of the overabundant adsorption of OH^- on the particle surfaces.

To summarize, at pH values of approximately 4 and 10.5, the Nd:YAG particle–water system is in its most stable configuration. It is empirically generally accepted that, below a critical value of ±30 mV, suspensions of lyophobic particles undergo changes in their dispersion state [39]. Therefore, the assessment of the electrokinetic properties of the Nd:YAG nanoparticle suspension on the amount of dispersant is based at pH = 10.5.

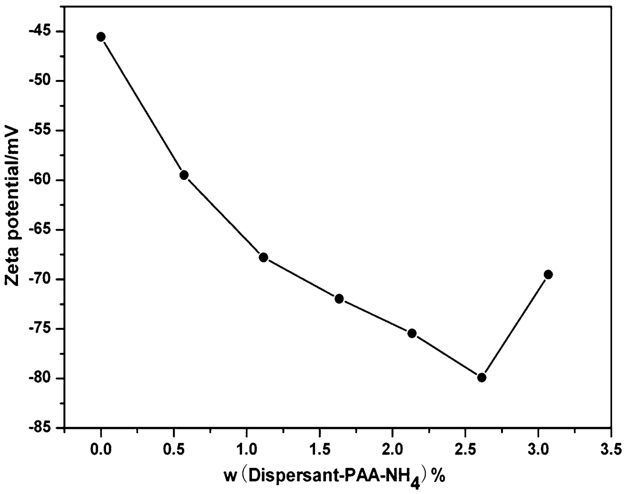

Fig. 3 Zeta potential for the Nd:YAG slurry as a function of NH_4PAA concentrations with pH = 10.5

Figure 3 shows the effect of concentration of the polymer NH_4PAA (w) on the zeta potential of the Nd:YAG particles in aqueous suspension with pH = 10.5. The addition of NH_4PAA lowers the zeta potential of the Nd:YAG nanoparticles in suspension in conformity with other oxide slurry systems. The zeta potential decreases with an increase in the amount of NH_4PAA. After reaching a minimum value at $w = 2.6$, it increases with additional amounts. The observation that dispersant addition increases the absolute value of the zeta potential indicates that the anion from the dissociated NH_4PAA is specifically absorbed on the particle surfaces. The functional groups of NH_4PAA are carboxylic acid (COO^-) groups in an aqueous solution as illustrated below:

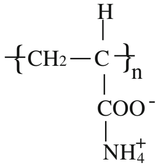

$$\left[CH_2 - \overset{\displaystyle H}{\underset{\underset{\displaystyle NH_4^+}{\displaystyle COO^-}}{C}} \right]_n$$

The ammonium carboxylate groups dissociate according to the reaction $RCOONH_4 = RCOO^- + NH_4^+$, which begins at pH >3.5; at pH ≥8.5 the polymer charge is negative with the degree of ionization approaching 1 [40]. Yu and Somasundaran [41] reported that at a pH of 10, NH_4PAA is fully ionized and adsorption is dominated by electrostatic interactions between the ionized sites on the polymer and the surface charged sites on the solid. In our experiment, the lowest zeta potential of the Nd:YAG slurry is about −80 mV when the concentration of NH_4PAA is 2.6 wt%, which indicates that this concentration is optimal for the addition of NH_4PAA in the YAG–water system. At this concentration, the adsorbed polymer layer on the Nd:YAG nanoparticles is close to a monolayer. This dispersant amount is considered the optimum one for stabilizing the suspension. Any further addition would not be adsorbed and would negatively affect the stability of the suspension with depletion and/or flocculation. Adding dispersant beyond what gives maximum coverage of the particles surfaces can lead to an excess of dispersant in solution, which in turn would exert a detrimental effect on the rheology for two possible reasons [16]: (1) acting as a free electrolyte, the ionic strength increases and thus screens the electrostatic forces on the particles, and (2) forming a complete monolayer or even a second adsorbed layer on the surface of particles with opposite orientation, thus completely reversing the surface charge. The former may lead to depletion flocculation as a result of the osmotic pressure created by the exclusion of unadsorbed polymer chains between two approaching particles that are coated by the dispersant. The latter, on the other hand, may lead to repulsive electrosteric particle interactions at higher dispersant concentrations.

Observation and measurement of sedimentation is another way of examining colloidal stability. A good dispersant will enable suspensions to maintain a cloudy state. Figure 4 shows the sedimentation behavior of 20 wt% Nd:YAG suspensions with various amounts of NH_4PAA added. For suspensions without any dispersants present, two distinct layers were observed after sedimentation. These two layers are a transparent aqueous layer on the top and a sediment layer at the bottom of the test tube. The relative height of the sediment layer (H_f/H_0) is 65.21%. The relative height of the sediment layer (H_f/H_0) increases with an increase in the amount added, reaches a maximum at a w value of about 2.6, and decreases with a further increase in the amount added. This result indicates that the optimal amount of NH_4PAA to be added for stabilizing the Nd:YAG nanoparticle slurry is about 2.6, which agrees with the results obtained from the zeta potential measurements (Fig. 3).

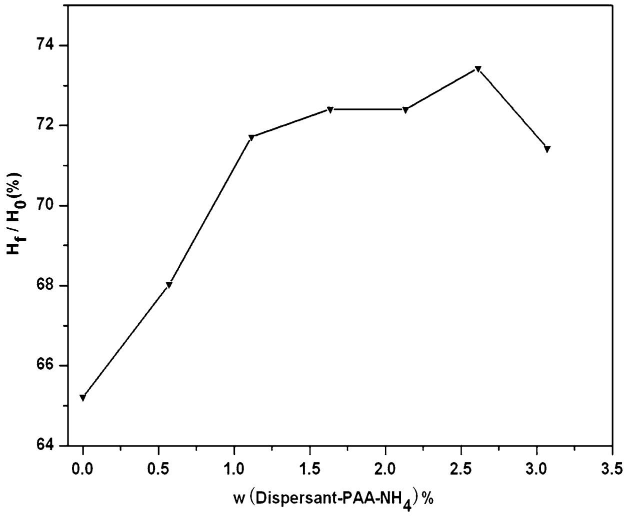

Fig. 4 The relative height of the sediment layer (H_f/H_0) as a function of NH_4PAA concentrations with 20 wt% solid content and pH = 10.5

It is understandable that the behavior of the slurry also depends on the concentration of the solid phase. The rheological behavior of YAG–NH_4PAA slip was studied by measuring the viscosity and shear stress at varying shear rates while maintaining different solid content (60, 65, 70 wt%) values at pH 10.5 with 2.6 wt% dispersant as shown in Fig. 5a, b. From the figure, it is clear that nearly Newtonian behavior was exhibited at the lower solid loadings of 60 and 65 wt%; whereas typical shear-thinning behavior that implies that no yield point exists [42–45] was observed at a solid loading of 70 wt%. The flow curves highlight the observation that the suspensions measured are "non-Newtonian systems", and present pseudo-plastic behavior. The flow curves at a solid loading of 70 wt% show the characteristics of a highly flocculated suspension with a yield stress of about 46 Pa and display a shear-thinning behavior. This is because liquid is immobilized in the inter-particulate pore spaces of the flocs and of the floc network of the suspension, resulting in an increased effective solid loading relative to the well-dispersed suspension. On application of a shear stress, shear-thinning flow results due to the breakdown of the flocculated structure and the release of entrapped liquid [46]. The viscosity value (solid content 60 wt%) is 33 mPa s at the maximum shear rate ($\gamma = 1000\ s^{-1}$). From the above results, suspensions based on a solid content of 60 wt% seem to have the best rheological behavior. Given the relationship between solid content and compact density, a solid content 65 wt% slurry is observed to be optimum.

Detailed characteristics of the nanosuspensions prepared under a range of different conditions are summarized in Table 1. From this table, it is clear that with the various casting parameters employed, the green density is different. It should be pointed out that the green body cracked when no dispersant was added in the process of ball milling. The highest green density of 57.7% of theoretical value ($2.6254\ g/cm^{-3}$) was obtained under optimum dispersion conditions. This result indicates that the addition of 2.6 wt% of the dispersant into the suspension with 65 wt% solid content leads to a green body with smaller pore diameter and one that is more compact. These results are in good agreement with the theoretical discussion above.

Figure 6 shows the microstructure of the fracture surfaces of green bodies under a range of different conditions. The condition of the various samples is identical to those in Table 1. A well-defined and more uniform microstructure can be observed as shown in Fig. 6a. Some flocculation

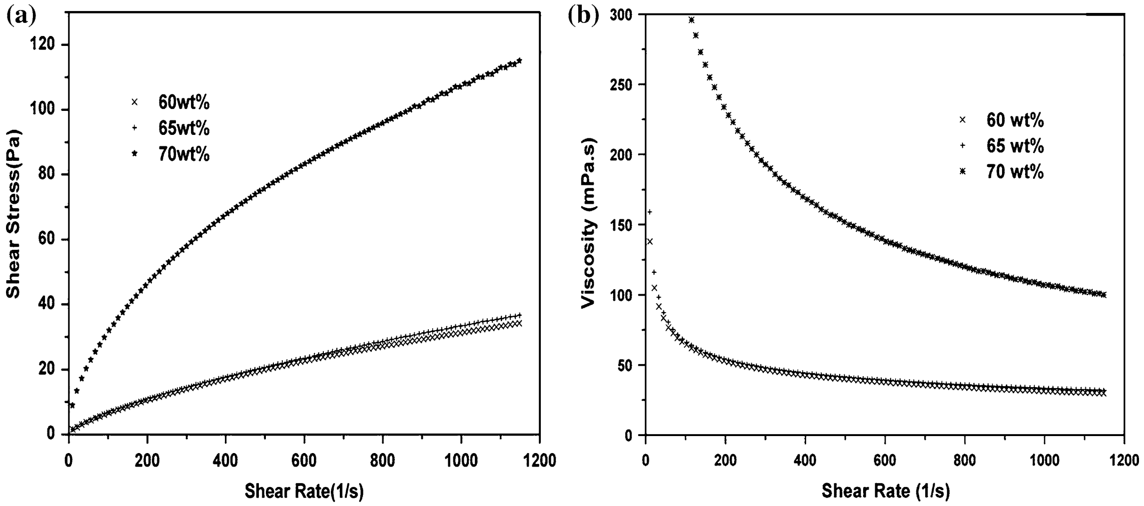

Fig. 5 Rheological behavior of concentrated (60, 65, 70 wt%) Nd:YAG suspensions at pH 10.5 with 2.6 wt% dispersant: **a** shear stress and **b** apparent viscosity versus shear rate

Table 1 Summary of the characteristics of the nanosuspensions prepared under a range of different conditions

Sample	Solid content (wt%)	pH	Dispersant (wt%)	Density (g/cm^3)
a	65	10.5	2.6	2.6254
b	65	12.5	2.6	2.4934
c	50	10.5	2.6	2.3025
d	50	10.5	0	Body cracks

among the particles can be observed again when the pH of the slurry is further increased (Fig. 6b). More pores were observed in the green body (Fig. 6c), indicating that a low solid content (50 wt%) is not sufficient to obtain a compact green body. Comparing the microstructure of the green bodies under a range of different conditions, an obvious difference in the compact density was observed among these samples. These results are in good agreement with the density measurement of the green bodies.

Conclusions

The investigation of the effect of pH on the electrokinetic properties of well-dispersed Nd:YAG nanopowder slurries shows that the zeta potential of the Nd:YAG nanoparticles depends on the pH of the slurry. At pH values of about 4, 8.5 and 10.5, the zeta potential takes on its maximum positive value, zero, and the maximum negative value, respectively. This variation indicates that at pH values of 4 and 10.5, the Nd:YAG nanoparticle slurry is very stable because of the great repulsive force between the nanoparticles caused by abundant H^+ or OH^- adsorbed on the nanoparticle surfaces. At pH = 8.5, the slurry is destabilized and easily agglomerates. The effect of adding NH_4PAA on the electrokinetic properties of the Nd:YAG nanoparticle slurry with pH = 10.5 illustrates that NH_4PAA can improve the stability of the slurry, and that the optimal amount is about 2.6 wt%. The rheological behavior of the Nd:YAG slip for different solid loading

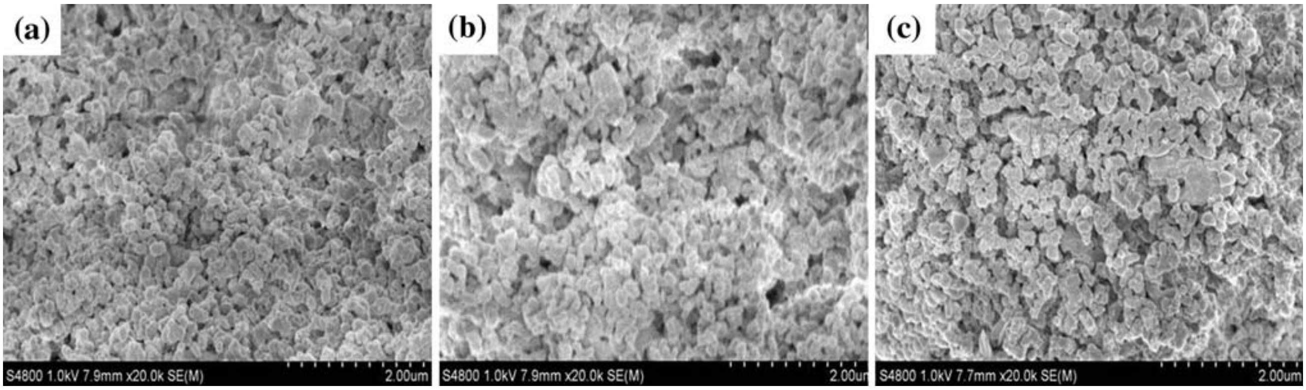

Fig. 6 SEM micrographs of fracture surfaces of slip cast Nd:YAG green bodies under a range of different conditions

(60–70 wt%) shows that slip with a solid loading of 65 wt% exhibits near-Newtonian behavior, whereas with higher solid loading the behavior changes to a shear-thinning mode. At the optimum pH value of 10.5 and at a dispersant concentration of 2.6 wt%, a 65 wt% solid loaded Nd:YAG slip was successfully slip cast to produce a dense and homogeneous microstructure ceramic.

Acknowledgements This research was supported by an NSFC (50872070, 50702031, Innovation Research Group, 50721002), the 973 Program of China (G2004CB619002, 2007CB613302), and the Program of Introducing Talents of Discipline to Universities in China (111 program). Thanks to R. I. Boughton at the Bowling Green State University for English revision on this paper.

References

1. Cockayne B (1985) J Less Common Met 144:119
2. Xu WL, Yue TM, Man HC (2008) J Mater Sci 43:942. doi: 10.1007/s10853-007-2208-3
3. Ahmed MA, Khalil AAI, Solyman S (2007) J Mater Sci 42:4098. doi:10.1007/s10853-006-1151-z
4. Corman GS (1991) Ceram Eng Sci Proc 12(9–10):1745
5. Li J, Wu YS, Pan YB, Kou HM, Shi Y, Guo JK (2008) Ceram Int 34:1675
6. Feng T, Shi JL, Jiang DY (2008) J Eur Ceram Soc 28(13):2539
7. Pradhan AK, Zhang K, Loutts GB (2004) Mater Res Bull 39:1291
8. Zhang HS, Han H, Su CH, Zhang HB, Hou ZX, Song Q (2007) Mater Sci Eng A 445–446:180
9. Li J, Wu YS, Pan YB, Guo JK (2006) J Non-Cryst Solids 352:2404
10. Vaidhyanathan B, Binner JGP (2006) J Mater Sci 41:5954. doi: 10.1007/s10853-006-0260-z
11. Ikesue A, Kinooshita T, Kamata K (1995) J Am Ceram Soc 78:1033
12. Even-Zur OT, Chaim R (2009) J Mater Sci 44:2063. doi: 10.1007/s10853-009-3300-7
13. Li X, Li Q (2008) Ceram Int 34:397
14. Kopylov YL, Kravchenko VB, Bagayev SN, Shemet VV, Komarov AA, Karban OV, Kaminskii AA (2009) Opt Mater 31(5):707
15. Esposito L, Piancastelli A (2009) J Eur Ceram Soc 29(2):317
16. Appiagyei KA, Messing GL, Dumm JQ (2008) Ceram Int 34(5):1309
17. Lu J, Ueda K, Yagi H, Yanagitani T, Akiyama Y, Kaminskii AA (2002) J Alloy Compd 341:220
18. Yagi H, Yanagitani T, Ueda K (2006) J Alloy Compd 421:195
19. Kochawattana S, Stevenson A, Lee SH, Ramirez M, Gopalan V, Dumm J, Castillo VK, Quarles GJ, Messing GL (2008) J Eur Ceram Soc 28(7):1527
20. Naito M, Fukuda Y, Yoshikawa N, Kamiya H, Tsubaki J (1997) J Eur Ceram Soc 17:251
21. Hirata Y (1997) Ceram Int 23:93
22. Li Y, Lin J, Gao JQ, Qiao GJ, Wang HJ (2008) Mater Sci Eng A 483–484:676
23. Kopylov YL, Kravchenko VB, Komarov AA, Lebedeva ZM, Shemet VV (2007) Opt Mater 29:1236
24. Hotta YJ, Omura NK, Sato K, Watari KJ (2007) J Eur Ceram Soc 27:753
25. Garrido LB, Agletti EF (2001) J Eur Ceram Soc 21:2259
26. Moreno R, Salomoni A, Stamenkovic I (1997) J Eur Ceram Soc 17:327
27. Tsetsekou A, Agrafiotis C, Milias A (2001) J Eur Ceram Soc 21:363
28. Rao RR, Roopa HN, Kannan TS (1999) Ceram Int 25:223
29. Houivet D, Fallah JE, Haussonne JM (2002) J Am Ceram Soc 85:321
30. Lu K, Kessler CS, Davis RM (2006) J Am Ceram Soc 89:2459
31. Li X, Liu H, Wang JY, Cui HM, Han F (2004) Opt Mater 25:407
32. Parfitt LR (1981) Dispersion of powders in liquids with special reference to pigments. Applied Science Publishers, London, UK
33. Wang JQ, Xu HY, Wang Y, Yue YL (2006) J Rare Earth 24:284
34. Wang HZ, Gao L, Shen ZJ, Nygren M (2001) J Eur Ceram Soc 21:779
35. Schindler PW (1981) Surface complexes at oxide–water interface. Ann Arbor Science Publishers, Ann Arbor, MI
36. Parks GA (1965) Chem Rev 65:177
37. Yoon RH (1979) J Colloid Sci 70:483
38. Parks GA, DeBruyn PL (1962) J Phys Chem 66:973
39. Everett DH (1988) Basic principles of colloid science. The Royal Society of Chemistry, Cambridge
40. Cesarano IIJ, Aksay IA, Bleier A (1988) J Am Ceram Soc 71:250
41. Yu X, Somasundaran P (1996) J Colloid Interface Sci 177:283
42. Bergström L (1994) In: Pugh RJ, Bergström L (eds) Surface and colloid chemistry, advanced processing. Marcel Dekker Inc, NY, USA, p 193
43. Barnes HA, Hutton JF, Walters K (1989) An introduction to rheology. Rheology Series 3. Elsevier Science Publishers B.V., Amsterdam, The Netherlands
44. Moreno R (2001) In: Messing GL (ed) The encyclopedia of materials. Science and technology.III. Structural materials. Ceramic processing. Elsevier Science, UK, p 8192
45. Moreno R (2005) Reología de suspensiones cerámicas, Biblioteca de Ciencias, vol 17. CSIC, Madrid, Spain
46. Sacks MD (1984) Am Ceram Soc Bull 63:1510